



# Lactobacillus Plantarum Promotes Wound Healing by Inhibiting the NLRP3 Inflammasome and Pyroptosis Activation in Diabetic Foot Wounds

Xiaojun Wang, Xu Li , Jianjun Liu, Yue Tao, Tao Wang, Limeng Li 

Vascular Surgery, Fudan University Zhongshan Hospital Qingpu Branch, Shanghai, People's Republic of China

Correspondence: Xu Li, Department of Vascular Surgery, Fudan University Zhongshan Hospital Qingpu Branch, 1158 East Park Road, Qingpu District, Shanghai, 201700, People's Republic of China, Email li.xu@qphospital.com

**Objective:** Diabetic foot ulcer (DFU) impairs the quality of life of diabetic patients and overburdens healthcare systems and society. It is crucial to comprehend the pathophysiology of DFU and develop effective treatment strategies. The aim of this study was to evaluate the therapeutic potential of Lactobacillus Plantarum (LP) on wound healing in DFU and to explore the underlying mechanisms.

**Methods:** To investigate the effects of LP on wound healing, human umbilical vein endothelial cells (HUVECs) were treated with advanced glycation end products (AGEs) and used to assess cell viability, migration, and pyroptosis using CCK-8, cell scratch, and flow cytometry. The levels of IL-1 $\beta$  and IL-18 were measured by ELISA. The expression of NLRP3, caspase-1 p20, and GSDMD-N was detected by Western blot. Additionally, NLRP3 inhibitor MCC950 was used to treat a diabetic rat model established by streptozotocin (STZ). Pearson correlation analysis was performed to analyze the relationship between LP and NLRP3, IL-1 $\beta$ , IL-18 in ulcer tissue.

**Results:** Our data mechanistically demonstrate that AGEs activate the NLRP3/Caspase-1/GSDMD pathway, leading to an increase in the levels of IL-1 $\beta$  and IL-18 and ultimately promoting cell pyroptosis. Furthermore, we identified that LP inhibits the effects of AGEs by downregulating NLRP3 inflammasome activity. LP facilitated wound healing in diabetic rats and resulted in decreased protein levels of NLRP3 and its downstream target caspase-1 p20. Finally, we observed a negative correlation between LP and NLRP3, IL-1 $\beta$ , IL-18 in diabetic foot skin tissue.

**Conclusion:** Our findings uncovered a novel role of LP in diabetic foot wound healing via regulation of the NLRP3 inflammasome, suggesting this link as a therapeutic target. In future research, it would be valuable to explore the signaling cascades involved in LP-mediated inhibition of NLRP3 inflammasome activation.

**Keywords:** lactobacillus plantarum, AGEs, NLRP3 inflammasome, diabetic foot wounds, pyroptosis

## Introduction

Diabetes mellitus (DM) is a growing public health concern with increasing prevalence worldwide, and one of the most common complications is diabetic foot ulcer (DFU).<sup>1,2</sup> DFU is caused by loss of glycemic control, peripheral neuropathy, and peripheral arterial disease.<sup>3</sup> DFU reduces the quality of life of DM patients and places a heavy burden on healthcare systems and society.<sup>4</sup> There is an urgent need to understand the pathogenesis of DFU and identify effective treatment strategies. It has been suggested that DFUs have the characteristics of chronic, non-healing wounds that exist in a persistent inflammatory state.<sup>5</sup> Additionally, hyperglycemia will elevate the level of advanced glycation end products (AGEs), which can induce endothelial cell injury and suppress wound healing.<sup>6,7</sup> Therefore, approaches to combat AGE-mediated effects appear to be promising therapeutics for DMF.

Chronic inflammation plays a critical role in the development of diabetic foot ulcers.<sup>8</sup> Activation of the pyrin domain containing 3 (NLRP3) inflammasome-related pathway, involving the disturbance in Nrf2 and the NF- $\kappa$ B, TLR receptor, and various stimuli inducing NLRP3 inflammasome assembly play a pivotal role in DFU healing.<sup>9</sup> NLRP3 inflammasome in response to hyperglycemia in diabetes leads to IL-1 $\beta$ -mediated inflammatory cascades. Elevated serum levels of IL-1 $\beta$  and IL-18

have been specifically linked to diabetic foot ulcers in patients with diabetes that fail to heal.<sup>10</sup> The NLRP3/Caspase-1/GSDMD pathway, which mediates the pyroptosis of vascular endothelial cells, has been recently shown to contribute to DFU and atherosclerosis.<sup>11,12</sup> Dysregulated NLRP3 inflammasome activation in macrophages has also been shown to create an imbalance of inflammatory reactions, disrupt insulin sensitivity, and delay angiogenesis and wound healing.<sup>13</sup> Therefore, sustained NLRP3 activation can perpetuate wound inflammation and result in refractory diabetic foot ulcers. Targeting the excessive activation of the NLRP3 inflammasome induced by hyperglycemic conditions may provide a novel treatment strategy for diabetic foot ulcers.

The pathophysiology of DFU is closely related to bacterial interactions on the surface of the skin, which can delay wound healing. The potential communication between the commensal microbiota and cells involved in cutaneous wound healing stimulates immune responses and helps maintain barrier function.<sup>14</sup> Bacterial interactions on the skin surface are vital to the pathophysiology of DFU and may control delayed wound healing.<sup>15</sup> *Lactobacillus Plantarum* (LP) is a probiotic that is widely distributed in nature with species diversity, but the potential benefits of strain-specific LP on wound healing are unknown. Some LP strains have important biological functions such as antioxidant, endotoxin control, anti-aging and immunity enhancement.<sup>16</sup> Some studies have shown that topical application of some strains of probiotic bacteria have good effects on the healing of cutaneous wounds.<sup>17,18</sup> Previous studies have explored the pathophysiological mechanism of LP. LP reduces oxidative stress and inhibits proinflammatory responses by downregulating the production of malondialdehyde (MDA), reactive oxygen species (ROS), tumor necrosis factor- $\alpha$  (TNF- $\alpha$ ), interleukin-6 (IL-6), and interleukin-1 $\beta$  (IL-1 $\beta$ ).<sup>19</sup> LP postbiotics decreased levels of NLRP3, Caspase-1 and apoptosis-associated speck-like protein containing a caspase recruitment domain (ASC) and suppressed various inflammatory cytokines against *Salmonella* infection.<sup>20</sup>

The potential of LP in wound healing has been examined in some studies. Nevertheless, there are still gaps and limitations in our understanding of LP's role in wound healing. The precise mechanisms underlying LP's wound healing effects remain unclear. Although several cytokines have been implicated, their precise interactions and regulatory networks remain elusive. The clinical applications of LP in wound care are still limited. Most studies have been conducted in vitro or in animal models, making the translation of these findings to humans challenging. With respect to clinical implications, further research is needed to confirm its efficacy and safety in clinical settings. The identification of specific signaling cascades involved in LP-mediated inhibition of NLRP3 inflammasome activation may provide valuable insights into the development of targeted therapies for wound care. Therefore, a precise understanding of the mechanism that LP promotes diabetic wound healing may be valuable in identifying potential therapeutic targets to improve clinical outcomes. In this study, we assessed the ability of LP to accelerate DFU healing by inhibiting the NLRP3 inflammasome and pyroptosis activation.

## Materials and Methods

### Cell Culture and Cell Transfection

Human umbilical vein endothelial cells (HUVECs) (American Type Culture Collection, Manassas, VA, USA) was used in this study. Cells were cultured in DMEM (Gibco) with 10% fetal bovine serum (FBS). To elevate the expression of NLRP3, the coding sequence was synthesized and cloned into pcDNA3.1(+) plasmid (Addgene, USA). Recombinant plasmids were transfected into HUVECs using Lipofectamine 2000 (Invitrogen, USA). Cells that were transfected with blank pcDNA3.1(+) plasmid were used as the negative control.

### Bacterial Culture

*L. plantarum* (ATCC 8014) was obtained from American Type Culture Collection (ATCC) and maintained at  $-80^{\circ}\text{C}$  as frozen stocks in de Man, Rogosa and Sharpe (MRS) broth (HKM Company, Guangdong, China) containing 10% glycerol. *L. plantarum* was cultivated in MRS agar broth at  $37^{\circ}\text{C}$  for 48h under anaerobic conditions and then centrifuged at  $4000\times g$  for 20 min. The cell pellet was washed twice and resuspended in sterile phosphate-buffered saline.

### Experimental Grouping

Treatments were divided into three groups as follows: In *group 1*, HUVECs were treated with different concentrations of AGEs (100, 200, and 400  $\mu\text{g/mL}$ ) for 48 h. In *group 2*, HUVECs were treated with 200  $\mu\text{g/mL}$  AGEs for 48 h with or without  $2\times 10^5$ ,  $2\times 10^6$ , or  $2\times 10^7$  CFU/mL *L. plantarum* (ATCC 8014) or 1  $\mu\text{M}$  NLRP3 inhibitor MCC950 (Selleck,

China) treatment for 24 h. In *group 3*, HUVECs were treated with 200 µg/mL AGEs for 48h with or without NLRP3 expression plasmid transfection along with  $2 \times 10^6$  CFU/mL *L. plantarum* treatment for 24h.

### Cell Counting Kit (CCK)-8 Assay

Following treatments, cells ( $5 \times 10^3$  cells/well) were plated in 96-well plates and cultured for 0, 12, 24, and 48 h. In each well, cells were incubated with 10 µL CCK-8 reagent (Dojindo, Kumamoto, Japan) for 1 h according to the manufacturer's protocol. Finally, the optical density was measured at 450 nm with a microplate reader (Bio-Rad, Hercules, USA).

### In vitro Wound Healing Assay

After treatment, cells ( $5 \times 10^5$  cells/well) were plated into 6-well plates and grown to 100% confluence. After 6-hour cell starvation, a sterile 200 µL pipette tip was used to scratch the monolayer, creating an artificial homogenous wound. Wound healing was then assessed at 0 h (before administration), 24 and 48 h.

### Assessment of Cell Death

Pyroptotic cell death was assessed by the staining of active Caspase 1 and propidium iodide (PI). In brief, 48 h treatment later, about  $5 \times 10^5$  HUVECs were inoculated into each well of a 6-well plate to obtain a confluence of 50%. Prepared cells were sequentially subjected to the incubation of 660-YVAD-FMK (ImmunoChemistry Technologies, Bloomington, MN, USA) following the instructions of the manufactures, the incubation with 10 µL PI (thermofisher) for 15 min, and then CytoFLEX flow cytometry analysis (Beckman Coulter Cytoflex S, Krefeld, Germany).

### Quantitative RT-PCR (qRT-PCR)

Total RNA was extracted using TRIzol reagent (Invitrogen, USA) and the cDNA was synthesized by using a PrimeScript kit (Takara Biotechnology, Dalian, China). The Quantitative RT-PCR using SYBR green PCR master mix (Applied Biosystems, Foster, CA, USA) was performed in an ABI 9700 real-time PCR system (Applied Biosystem). Gene expression was normalized to GAPDH. The applied primer sequences were: NLRP3-F: 5'-ATGTGGGGGAGAATGCCTTG-3'; NLRP3-R: 5'-TTGTCTCCGAGAGTGTGTC-3'; GAPDH-F: 5'-AATCCCATCACCATCTTC-3'; and GAPDH-R: 5'-AGGCTGTTGTCATCTTC-3'. We determined mRNA fold-changes using the  $2^{-\Delta\Delta CT}$  method.

### Western Blot

Total protein was extracted using Radio Immunoprecipitation Assay (RIPA) lysis buffer (JRDUN Biotechnology Co. Ltd, Shanghai, China; BYL40825). Proteins were separated in sodium dodecyl sulfate polyacrylamide gel electrophoresis (SDS-PAGE) and transferred to polyvinylidene fluoride (PVDF) membrane. The membrane was blocked with 5% skim milk and then incubated with primary antibodies against NLRP3 (Proteintech Group, Inc., Rosemont, IL, USA; 19,771-1-AP), ASC (Abcam, Cambridge, MA, USA; ab151700), Caspase-1 p20 (Invitrogen; PA599390), GSDMD-N (Abcam; ab255983), and GAPDH (Abcam: 4366), followed by incubation with horse radish peroxidase-conjugated secondary antibodies (ZSGB-BIO, Beijing, China; ZB-2301, ZB-2305). Prestained protein ladders (Gene-Protein Link, Beling, China, P06M01, P06M02) were used. The content of protein was detected by enhanced chemiluminescence system (Bio-Rad, USA).

### Animal Models

A total of 48 male SD rats (4–6 weeks, 180–200g) were used in this study. They were randomized into four groups: in control group, rats received saline; in diabetic group, rats were intraperitoneally administrated 60 mg/kg streptozotocin (STZ) citrate buffer to induce diabetes, followed by skin wounds; in diabetes + MCC950 group, STZ rats with skin wounds were intraperitoneally treated with 10 mg/kg MCC950; in diabetes + *L. plantarum* group, STZ rats with skin wounds were treated with  $2 \times 10^6$  CFU/mL *L. plantarum*. The diabetes was established when the blood glucose of rats exceeded 16.7 mM after 48-hour of STZ administration. The skin wounds (1.3×1.3cm) were made using a scissor on the midback of rats at 72h after STZ administration. A digital camera was used to photograph wounds on day 0, day 7, and day 14. Image-pro plus 6.0 software (Media Cybernetics, Inc.) was used to quantify wound bed sizes, and wound healing was measured as follows: wound healing (%) =  $(1 - W_r) / W_i \times 100\%$ , where  $W_i$  is the initial wound area at day 0,

while  $W_r$  is the residual wound area at day 7 and day 14 post-injury. The all animal experiments were performed with the approval of the institutional animal care and use committee of Hospital.

## Hematoxylin and Eosin (HE) Staining

Wound tissues on day 0, 7 and day 14 were fixed with 4% paraformaldehyde. HE staining was performed as previously described. Digital images were captured at 200 $\times$  magnification using an Olympus BX51 microscope equipped with an Olympus DP71 charge-coupled device camera (Olympus Corporation, Japan). Image analyses were performed by blinded operators.

## Clinical Specimens of Diabetic Foot Ulcer

A total of 50 skin tissues of patients with diabetic foot ulcer were collected in Hospital, which included 25 lesions with 1–2 diabetic ulcer severity score (DUSS) and 25 lesions with 3–4 DUSS. Written informed consent was obtained from patients. This study was approved by the Ethics Committee of Hospital.

## Elisa

Corresponding ELISA kits from Nanjing Jiancheng Bioengineering Institute were adopted to analyze the secretion of IL-1 $\beta$  and IL-18 in HUVECs supernatants and wound tissues of rats and patients, respectively.

## DNA Copy Analysis

Bacterial DNA in the wound tissues from different groups was extracted by a Bacterial Genomic DNA Extraction Kit (TIANGEN BIOTECH (BEIJING)Co., LTD., China) according to the manufacturer's instructions. DNA copy number of *L. plantarum* in different groups of wound tissues was measured with qRT-PCR using the Hieff<sup>®</sup> qPCR SYBR Green Master Mix (Yeasen Biotechnology (Shanghai) Co., Ltd., China) and then analyzed with the ABI-7300 System (Applied Biosystems, Carlsbad, CA, USA). The sequences of primers used were as follows: *L. plantarum* ACTGTGGCTTGATTGTTTG (F), AGCTGGTTATATGGCTTAAGG (R). pGM-T plasmids containing the *L. plantarum* DNA sequence were constructed by GENERAL BIO (Chuzhou, China) and used as standards for qRT-PCR reactions.

## Ethical Statement

The study was conducted in accordance with the Declaration of Helsinki (as revised in 2013) and was approved by the regional ethics committee in Qingpu Branch of Zhongshan Hospital, Fudan University (approval number, 2021–13). All patients provided informed consent. The animal study was reviewed and approved by the Institute Research Ethics Committee at the Qingpu Branch of Zhongshan Hospital, Fudan University (approval number, 2020–366), in compliance with USA Institute for Laboratory Animal Research (ILAR) Guide for the care and use of animals.

## Statistical Analysis

All statistical analyses were conducted on GraphPad Prism 8.4.2. Experiments were conducted in triplicates and data were presented as mean  $\pm$  standard deviation (SD). Group comparisons were performed by Student's *t*-test or one-way ANOVA followed by Tukey's post-multiple test. The correlation between *L. plantarum* and NLRP3, IL-1 $\beta$ , and IL-18 was analyzed by Pearson correlation analysis. The *p*-value <0.05 was statistical significance.

## Results

3.1 AGEs inhibit cell viability and promote cell pyroptosis and NLRP3 inflammasome activation in HUVECs. We first confirmed the functions of AGEs on HUVECs. After a 48-hour treatment with AGEs (100, 200, and 400  $\mu$ g/mL), cell viability was observed to decrease (Figure 1A). Subsequently, the migration ability of the cells was significantly diminished upon AGE treatment (Figure 1B and C). To examine the impact of AGEs on cell pyroptosis, flow cytometry analysis was conducted. The results showed a significant increase in cell pyroptosis after AGE treatment (Figure 1D and E). Furthermore, ELISA results demonstrated a notable elevation in the levels of IL-1 $\beta$  and IL-18 following AGE



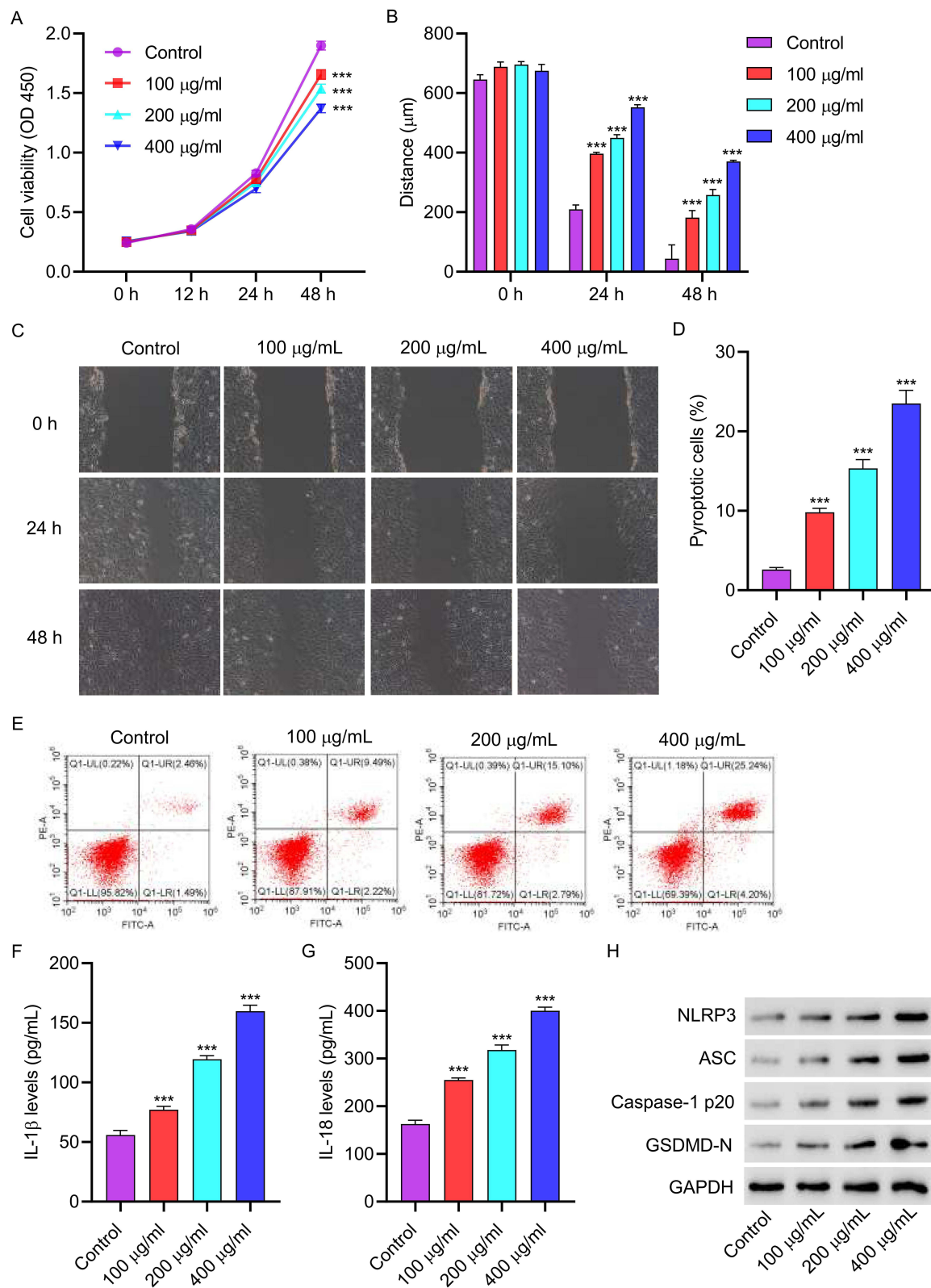


**Figure 1** AGEs inhibit cell viability and promote cell pyroptosis and NLRP3 inflammasome activation in HUVECs. HUVECs were treated with different concentrations of AGEs for 48 hours. **(A)** cell proliferation activity was detected by CCK8. **(B and C)** cell migration was detected by scratch test. **(D and E)** cell pyroptosis was detected by flow cytometry. **(F and G)** the level of IL-1β and IL-18 was detected by ELISA. **(H)** The expressions of NLRP3, ASC, Caspase-1p20 and GSDMD-N were detected by Western blot. \*\*\* $P < 0.001$  vs control.

treatment (Figure 1F and G). Moreover, Western blot analysis revealed augmented expressions of NLRP3, ASC, Caspase-1p20, and GSDMD-N in HUVECs treated with AGEs (Figure 1H).

3.2 LP inhibits the effects of AGEs on cell viability, pyroptosis and NLRP3 inflammasome activation in HUVECs. We investigated whether LP could mitigate the promotion of cell pyroptosis by AGEs. In the presence of LP at varying concentrations ( $2 \times 10^5$ ,  $2 \times 10^6$ , or  $2 \times 10^7$  CFU/mL) and 200  $\mu$ g/mL AGEs, cell viability was observed to increase (Figure 2A). Furthermore, at higher concentrations of LP, cell migration was significantly improved (Figure 2B and C). Flow cytometric analysis demonstrated that LP treatment significantly inhibited cell pyroptosis (Figure 2D and E). Additionally, ELISA results indicated that treatment with LP led to a decrease in the levels of IL-1 $\beta$  and IL-18 (Figure 2F and G). Furthermore, Western blot analysis revealed reduced expressions of NLRP3, ASC, Caspase-1p20, and GSDMD-N in HUVECs treated with LP (Figure 2H).

3.3 NLRP3 overexpression inhibits the effects of LP on AGEs-induced HUVECs. To further investigate the role of LP in inhibiting NLRP3 inflammasome activation induced by AGEs, we conducted experiments involving the overexpression and underexpression of NLRP3 in HUVECs to assess their impact on cellular behavior. HUVECs were transfected with a NLRP3 overexpression vector, and successful transfection was confirmed through PCR and Western blot analysis (Figure 3A and B). Subsequently, HUVECs were treated with 200  $\mu$ g/mL of AGEs alone or in combination with NLRP3 overexpression plasmids for 48 hours, with the simultaneous addition of  $2 \times 10^6$  CFU/mL of LP. The cell viability of HUVECs with NLRP3 overexpression was significantly decreased compared to those treated with LP alone, as determined by CCK assays (Figure 3C). Additionally, the migration ability of the cells was significantly impaired after overexpressing NLRP3 (Figure 3D and E). Flow cytometry analysis revealed that NLRP3 overexpression led to increased pyroptosis compared to cells treated with LP alone (Figure 3F and G). ELISA assays demonstrated that NLRP3 overexpression resulted in elevated levels of IL-1 $\beta$  and IL-18 (Figure 3H and I). Furthermore, Western blot analysis revealed that NLRP3 overexpression increased the expressions of ASC, Caspase-1p20, and GSDMD-N in HUVECs (Figure 3J).

3.4 The NLRP3 inhibitor MCC950 attenuated AGEs-induced cell pyroptosis in HUVECs. HUVECs were treated with 200  $\mu$ g/mL of AGEs for 48 hours, along with the addition of 1  $\mu$ M NLRP3 inhibitor MCC950. Inhibiting NLRP3 in HUVECs resulted in an increase in cell viability compared to cells treated with AGEs alone (Figure 4A). Moreover, cell migration was significantly increased after MCC950 treatment (Figure 4B and C). Flow cytometry analysis revealed that knocking down NLRP3 reversed the pyroptosis effects caused by AGEs (Figure 4D and E). ELISA assays showed that underexpressing NLRP3 led to a notable decrease in the levels of IL-1 $\beta$  and IL-18 when compared to cells treated with AGEs only (Figure 4F and G). Consistent with the cellular data, Western blot analysis revealed that MCC950 treatment decreased the expressions of NLRP3, ASC, Caspase-1p20, and GSDMD-N in HUVECs (Figure 4H). These results suggest that NLRP3 inflammasome plays a key role in AGEs-induced cell pyroptosis in HUVECs.

3.5 LP facilitates wound healing in diabetic rats. To establish the biological relevance of these findings, we examined the effects of inhibiting NLRP3 inflammasome on wound healing using diabetic rats as a model. The rats were treated with either 10 mg/kg of MCC950 or  $2 \times 10^6$  CFU/mL of LP for 14 days. To test the function of LP in wound healing, skin biopsy punch was initiated, and representative images of wounds from control, STZ, MCC950 and LP treatment groups were collected at day 0, 7, and 14. As shown in Figure 5A and B, wound healing in STZ-treated rats was slower compared to control. However, STZ treatment with MCC950 or LP accelerated wound healing (Figure 5A and B), suggesting that inhibition of NLRP3 inflammasome promotes wound healing. These results were supported by hematoxylin and eosin staining of tissues, in which MCC950 or LP treatment in STZ-treated rats resulted in accelerated wound repair (Figure 5C). Furthermore, as shown by ELISA, treatment with MCC950 or LP dramatically decreased the concentrations of IL-1 $\beta$  and IL-18 (Figure 5D and E). Consistent with our observations in vitro, Western blot analysis revealed that MCC950 or LP treatment decreased the expressions of NLRP3, ASC, Caspase-1p20, and GSDMD-N in diabetic rats (Figure 5F). All together, these data demonstrate that LP facilitates wound healing in vivo.

3.6 Correlation between LP and NLRP3, IL-1 $\beta$ , or IL-18 in patients with diabetic foot ulcer. Finally, to explore the correlation between the expression of LP and NLRP3, IL-1 $\beta$  or IL-18 in vivo, skin tissues were collected from 25 patients presenting DUSS 1–2 and DUSS 3–4. The expressions of LP and NLRP3, IL-1 $\beta$  and IL-18 were detected by Real-time PCR. Interestingly, we found that the mRNA expressions of LP were significantly decreased in DUSS 3–4 group compared with

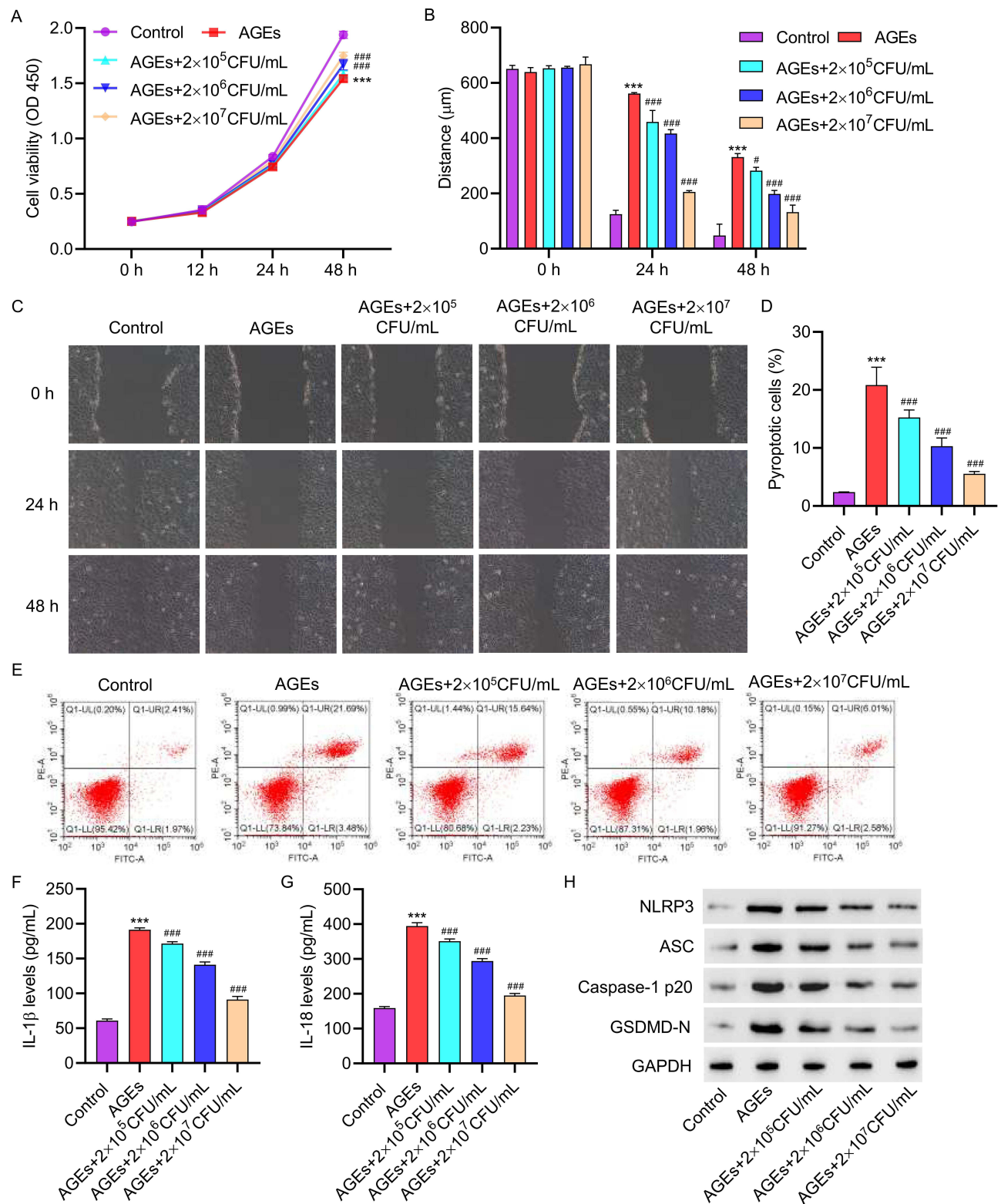


**Figure 2** *L. plantarum* inhibits the effects of AGEs on cell viability, pyroptosis and NLRP3 inflammasome activation in HUVECs. Treatment HUVECs with 200  $\mu$ g/mL of AGEs for 48 hours, with concomitant intervention of  $2 \times 10^5$ ,  $2 \times 10^6$ , or  $2 \times 10^7$  CFU/mL of *L. plantarum* for 24 hours. (A) Cell proliferation activity was detected by CCK8 assay. (B and C) Cell migration was detected by scratch assay. (D and E) Cell pyroptosis was detected by flow cytometry. (F and G) The levels of IL-1 $\beta$  and IL-18 were detected by ELISA. (H) The expression of NLRP3, ASC, Caspase-1 p20, and GSDMD-N was detected by Western blot. \*\*\* $P < 0.001$  vs control; # $P < 0.05$ , ### $P < 0.001$  vs AGEs.

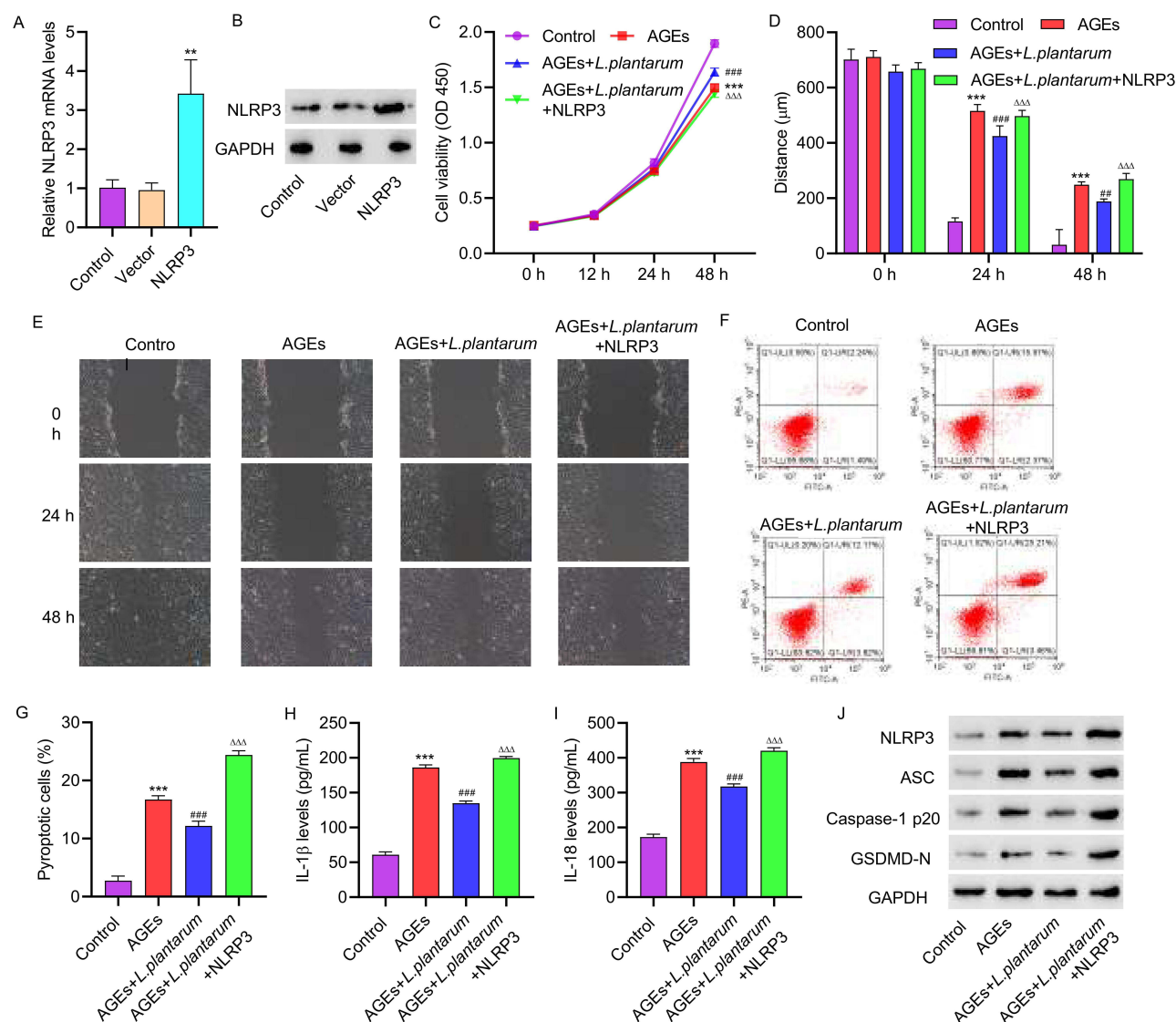


**Figure 3** NLRP3 overexpression inhibits the effects of *L. plantarum* on AGEs-induced HUVECs. NLRP3 overexpression vector was constructed and transfected into HUVECs. HUVECs were treated with 200 μg/mL of AGEs alone or in combination with NLRP3 overexpression plasmids for 48 hours, with concomitant intervention of  $2 \times 10^6$  CFU/mL of *L. plantarum* for 24 hours. NLRP3 expression was detected by qRT-PCR (A) and Western blot (B). (C) Cell proliferation activity was detected by CCK8 assay. (D, E) Cell migration was detected by scratch assay. (F, G) Cell pyroptosis was detected by flow cytometry. (H, I) The levels of IL-1β and IL-18 were detected by ELISA. (J) The expression of NLRP3, ASC, Caspase-1 p20, and GSDMD-N was detected by Western blot. \*\* $P < 0.01$ , \*\*\* $P < 0.001$  vs control; ### $P < 0.01$ , #### $P < 0.001$  vs AGEs; ΔΔΔ $P < 0.001$  vs AGEs+*L. plantarum*.

DUSS 1–2 group (Figure 6A), while the mRNA expressions of NLRP3, IL-1β, IL-18 were obviously increased in Severe staging (Figure 6B–D). Furthermore, Pearson correlation scatter plots in skin tissues of patients with diabetic foot ulcer strongly supported negative correlation between LP and NLRP3, IL-1β, IL-18 in diabetic foot skin tissue (Figure 6E–G). Taken together, these findings suggested that LP could down-regulate NLRP3, IL-1β or IL-18 those induced by AGEs.

## Discussion

In this study, we found that AGEs restricted cellular viability and promoted cell pyroptosis and NLRP3 inflammasome activation in HUVECs. LP mitigated the impact of AGEs on cell viability, pyroptosis, and NLRP3 inflammasome activation in HUVECs. Additionally, we determined that the NLRP3 inflammasome played a key role as a target and intermediary in the AGE-induced effects. Overexpression of NLRP3 negated the impact of LP on AGE-induced HUVECs. Furthermore, we underscored the physiological relevance of our findings by demonstrating that LP facilitated



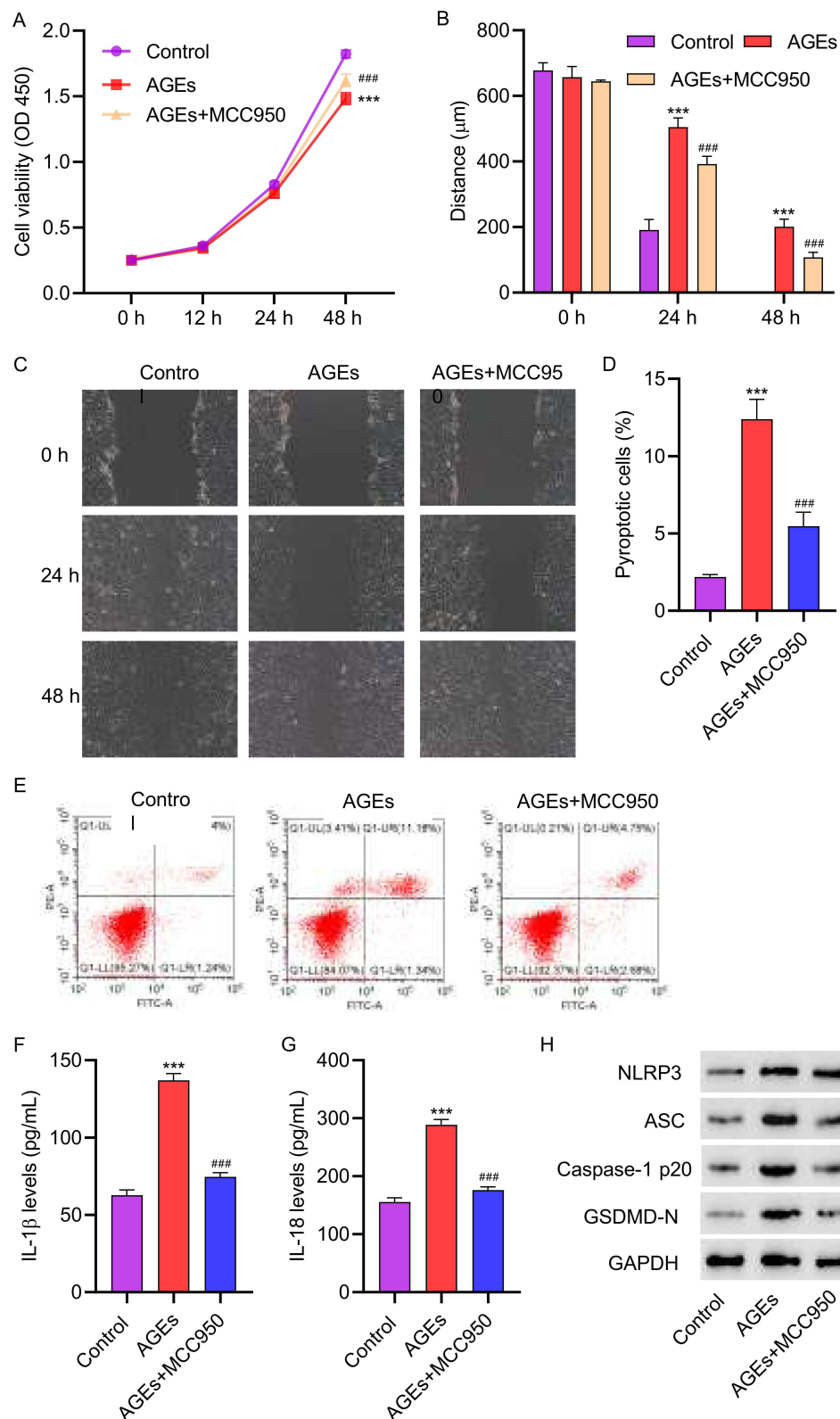


**Figure 4** The NLRP3 inhibitor MCC950 attenuated AGEs-induced cell pyroptosis in HUVECs. HUVECs were treated with 200 μg/mL AGEs for 48 hours, with concomitant intervention of 1 μM NLRP3 inhibitor MCC950 for 24 hours. **(A)** Cell proliferation activity was detected by CCK8 assay. **(B and C)** Cell migration was detected by scratch assay. **(D and E)** Cell pyroptosis was detected by flow cytometry. **(F and G)** The levels of IL-1β and IL-18 were detected by ELISA. **(H)** The expression of NLRP3, ASC, Caspase-1p20, and GSDMD-N was detected by Western blot. \*\*\* $P < 0.001$  vs control; ### $P < 0.001$  vs AGEs.



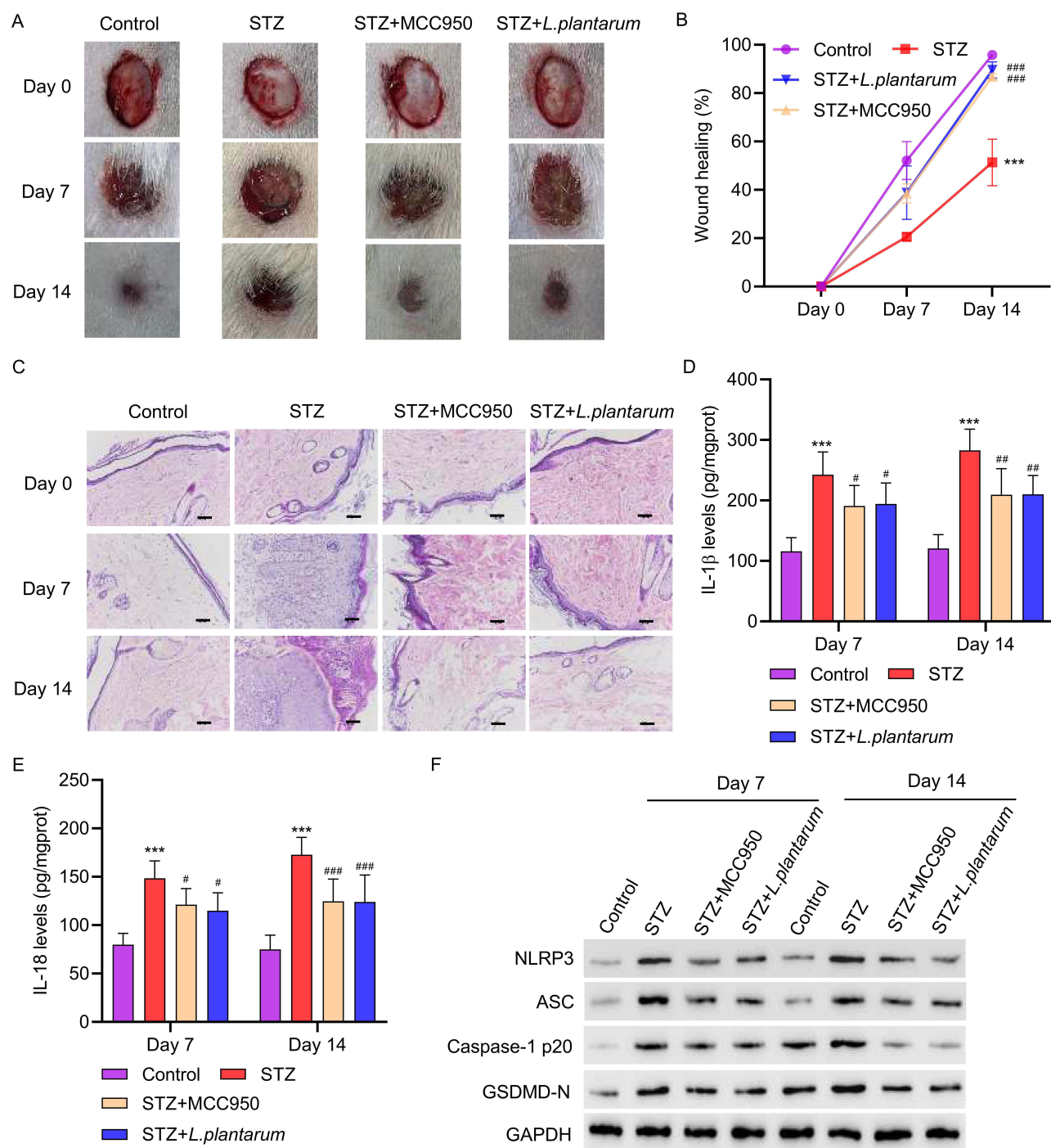


**Figure 5** *L. plantarum* facilitates wound healing in diabetic rats. SD rats were intraperitoneally injected with 60 mg/kg STZ to establish a diabetic rat model. The skin wounds (1.3×1.3cm) were made using a scissor on the midback of rats at 72h after STZ administration. The rats were treated with either 10 mg/kg of MCC950 or 2×10<sup>6</sup> CFU/mL of *L. plantarum* for 7 or 14 days. (**A** and **B**) photographs of wounds were taken to calculate the healing rate. (**C**) Pathological changes of the ulcer tissue were analyzed by HE staining (scale bar, 50  $\mu$ m). (**D** and **E**) The levels of IL-1 $\beta$  and IL-18 were detected by ELISA. (**F**) The expression of NLRP3, ASC, Caspase-1 p20, and GSDMD-N was detected by Western blot. \*\*\* $P$ <0.001 vs control; # $P$ <0.05, ### $P$ <0.01, #### $P$ <0.001 vs STZ.

wound healing in vivo diabetic rats, suggestive of its therapeutic potential. Lastly, we detected a negative correlation between LP and NLRP3, IL-1 $\beta$ , or IL-18 in skin wound tissues of DFU patients. Collectively, these findings suggest that LP may alleviate inflammatory response by downregulate NLRP3 inflammasome, IL-1 $\beta$ , and IL-18 induced by AGEs to promotes wound healing (Figure 7).

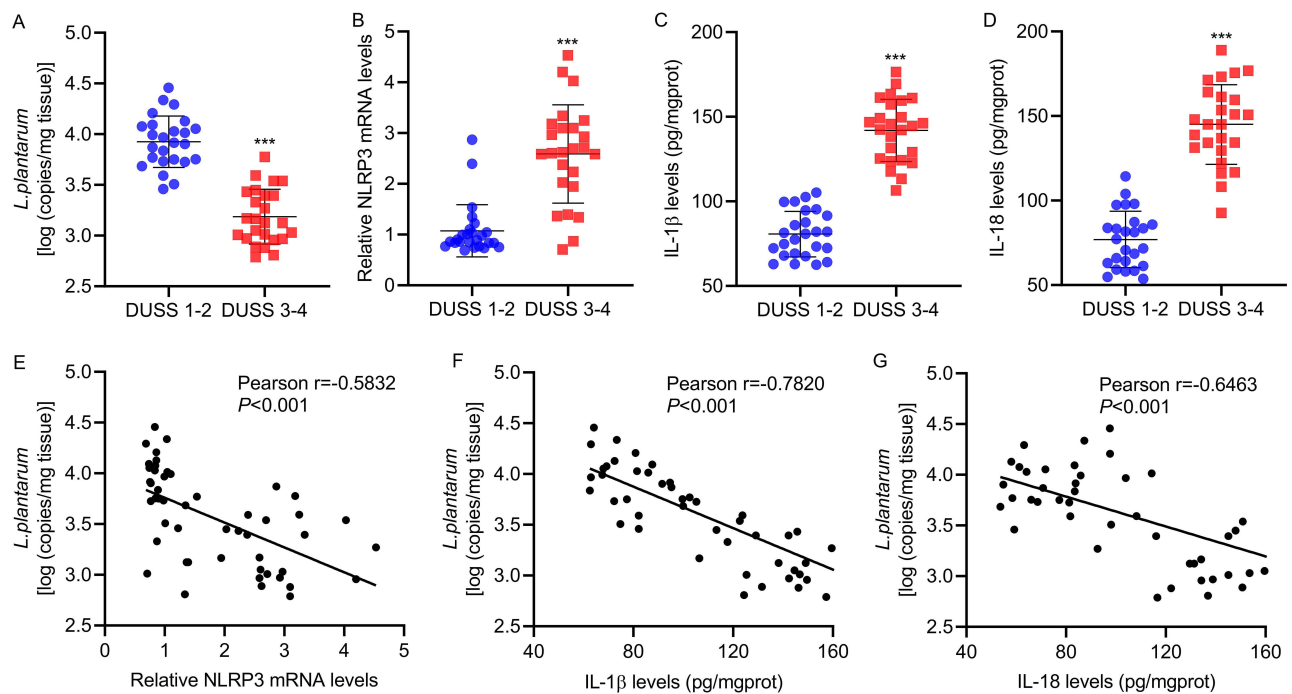


**Figure 6** Correlation between *L. plantarum* and NLRP3, IL-1 $\beta$ , or IL-18 in patients with diabetic foot ulcer. Skin tissues were collected from 25 patients presenting DUSS 1–2 and DUSS 3–4. (A) *L. plantarum* and (B) NLRP3 expression in ulcer tissues were detected by qRT-PCR. (C, D) IL-1 $\beta$  and IL-18 expression in ulcer tissues were detected by ELISA. (E–G) Pearson correlation analysis between *L. plantarum* and NLRP3, IL-1 $\beta$ , and IL-18. \*\*\* $P < 0.001$  DUSS 1–2 vs DUSS 3–4.

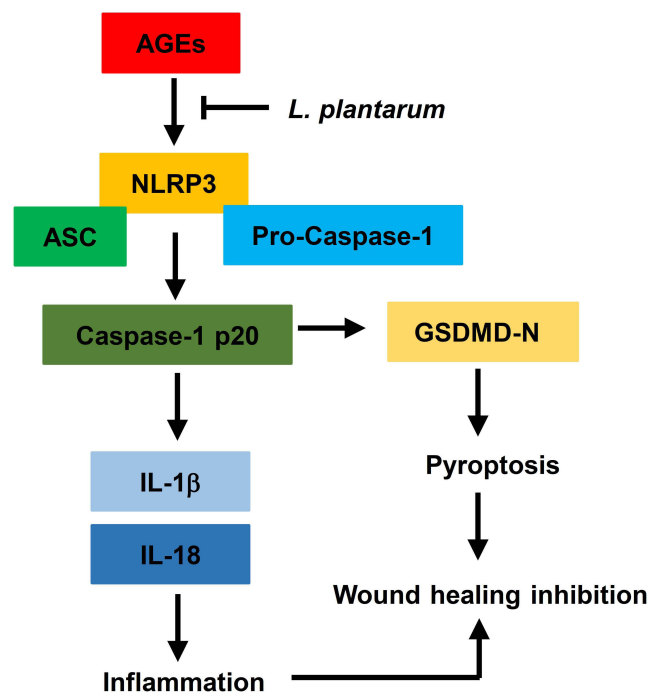


**Figure 7** *L. Plantarum* promotes diabetic wound healing by inhibiting the effects of AGEs and NLRP3 inflammasome activation.

Currently, many research studies have been exploring molecules or drugs that can inhibit the NLRP3 inflammasome, which helps reduce inflammation in diabetic foot ulcers and promote wound healing. It was discovered by SF, Yang et al that disulfiram accelerates diabetic foot ulcer healing by inhibiting neutrophil extracellular trap formation, suppressing

the NLRP3/Caspase-1/GSDMD pathway.<sup>21</sup> Laura Acciari et al conducted a study on the Caribbean's nine plants that promote wound healing in diabetes, particularly highlighting the role of five polyphenols. The use of medicinal plants and natural compounds can improve diabetic wound healing by directly targeting oxidative stress and transcription factor Nrf2 involved in antioxidant response or ROS-affected mechanisms such as NLRP3 inflammasome modulation, macrophage polarization, and metalloproteinase expression or activation.<sup>22</sup> Additionally, Bletilla striata polysaccharide and USP30 inhibitor MF-094 can promote DFU healing through inhibition of hyperglycemia-activated NLRP3 inflammasome.<sup>23,24</sup> Phenylpyruvate is ingested into macrophages and increase palmitoylation of the NLRP3 protein. Increased NLRP3 palmitoylation can promote NLRP3 inflammasome activation and the release of inflammatory factors, such as interleukin (IL)-1 $\beta$ . Therefore, reducing phenylpyruvate via dietary phenylalanine restriction relieves uncontrolled inflammation and benefits diabetic wounds.<sup>13</sup>

Probiotic is established to promote wound healing via antimicrobial activity, inhibition of pathogenic toxins, immunomodulation, and anti-inflammatory actions. Simarjot et al have developed a wound dressing that incorporates curcumin loaded solid lipid nanoparticles (CSLNs) and LP. This dressing was found to be equally effective as the silver nanoparticle-based commercial hydrogel dressing.<sup>25</sup> Jung Suk Kim developed a LP-loaded dual-layer wound dressing (DLD) with excellent wound recovery and mechanical properties. This DLD containing LP accelerated wound recovery with complete re-epithelialization.<sup>26</sup> The protein-rich fraction from LP USM8613 can exert wound healing properties via direct inhibition of *S. aureus* and promoted innate immunity.<sup>27</sup> YC Chuang found that the topical application of the ethanol extract of LP TWK10-fermented soymilk is beneficial for enhancing wound healing and for the closure of diabetic wounds.<sup>28</sup> The results of the current study suggest that LP can enhance diabetic wound healing through modulation of inflammation. In vivo diabetic wound healing experiments were conducted using Wistar rats treated with LP. The altered mRNA levels of inflammatory cytokines were observed in wound sites following treatment with LP.<sup>17</sup> Panagiotou D et al applied topically the LP UBLP-40 to promote wound healing and discovered that LP exhibited a robust anti-inflammatory effect.<sup>29</sup> LP also plays a therapeutic role in other diseases by inhibiting the NLRP3 inflammasome. LP DP189 activated the expression of nuclear factor erythroid 2-related factor (Nrf2)/ARE and PGC-1 $\alpha$  pathways and suppressed the NLRP3 inflammasome to delay the neurodegeneration of Parkinson's disease.<sup>30</sup> Lactobacillus Plantarum NC8 and its metabolite acetate alleviate type 1 diabetes via inhibiting NLRP3.<sup>31</sup>

In future studies, it would be interesting to explore the specific mechanisms by which LP regulates cell viability. Understanding the molecular pathways and signaling molecules involved in LP-mediated cell protection would provide valuable insights into its therapeutic potential in diabetic foot wounds. Furthermore, it would be valuable to identify the downstream regulators of LP and further explore the signaling cascades involved in LP-mediated inhibition of NLRP3 inflammasome activation. Understanding the molecular targets and pathways through which LP exerts its effects would aid in the development of targeted therapies for AGEs-induced inflammation. Next-generation sequencing and the advancement of bioinformatics pipelines have the potential to significantly enhance our understanding of the microbiome-skin axis involved in diabetic wound healing through a highly sophisticated approach. Overall, this study highlights the potential of LP as a therapeutic agent for AGEs-induced inflammation, but further research is needed to fully elucidate the underlying mechanisms and therapeutic implications.

## Conclusions

In summary, our findings have revealed a novel role of LP in the control of inflammation in diabetic foot ulcers. The research has shown that LP can suppress the activation of the NLRP3 inflammasome and pyroptosis, which are triggered by AGEs, to promote wound healing. Therefore, LP may represent a promising therapeutic target for the treatment of diabetic foot ulcers. Additional research is required to confirm the effectiveness and safety of LP in clinical settings, and well-structured clinical trials will play a significant role in future endeavors.

## Acknowledgments

This study was funded by the Shanghai Municipal Health Commission (202040062).

## Author Contributions

All authors contributed to data analysis, the drafting or revision of the article, have agreed on the journal in which the article will be submitted, gave final approval for the version to be published, and agree to be accountable for all aspects of the work.

## Disclosure

The authors report no conflicts of interest in this work.

## References

- Schaper NC, van Netten JJ, Apelqvist J, et al. Practical guidelines on the prevention and management of diabetic foot disease (IWGDF 2019 update). *Diabetes Metab Res Rev*. 2020;36(Suppl S1):e3266. doi:10.1002/dmrr.3266
- Lim JZ, Ng NS, Thomas C. Prevention and treatment of diabetic foot ulcers. *J R Soc Med*. 2017;110:104–109.
- Armstrong DG, Boulton AJM, Bus SA. Diabetic foot ulcers and their recurrence. *N Engl J Med*. 2017;376(24):2367–2375.
- Cawich SO, Islam S, Hariharan S, et al. Trends and determinants of costs associated with the inpatient care of diabetic foot ulcers. *J Vasc Surg*. 2014;60(5):1247–1254.
- Salazar JJ, Ennis WJ, Koh TJ. Diabetes medications: impact on inflammation and wound healing. *J Diabet Complicat*. 2016;30:746–752.
- Shaikh-Kader A, Houreld NN, Rajendran NK, et al. The link between advanced glycation end products and apoptosis in delayed wound healing. *Cell Biochem Funct*. 2019;37:432–442.
- Cheng M, Yang Z, Qiao L, et al. AGEs induce endothelial cells senescence and endothelial barrier dysfunction via miR-1-3p/MLCK signaling pathways. *Gene*. 2023;30(851):147030.
- Littig JPB, Moellmer R, Estes AM, et al. Increased population of cd40+ fibroblasts is associated with impaired wound healing and chronic inflammation in diabetic foot ulcers. *J Clin Med*. 2022;11(21):6335.
- Ding Y, Xiaofeng D, Zhang H, et al. Relevance of NLRP3 inflammasome-related pathways in the pathology of diabetic wound healing and possible therapeutic targets. *Oxid Med Cell Longev*. 2022;2022:9687925.
- Huang W, Jiao J, Liu J, et al. MFG-E8 accelerates wound healing in diabetes by regulating "NLRP3 inflammasome-neutrophil extracellular traps" axis. *Cell Death Discov*. 2020;6:84.
- Sun X, Wang X, Zhao Z, et al. Paeniflorin inhibited nod-like receptor protein-3 inflammasome and NF-κB-mediated inflammatory reactions in diabetic foot ulcer by inhibiting the chemokine receptor CXCR2. *Drug Dev Res*. 2021;82(3):404–411.
- Yao F, Jin Z, Zheng Z, et al. HDAC11 promotes both NLRP3/caspase-1/GSDMD and caspase-3/GSDME pathways causing pyroptosis via ERG in vascular endothelial cells. *Cell Death Discov*. 2022;8(1):112.
- Dongming L, Cao X, Zhong L, et al. Targeting phenylpyruvate restrains excessive NLRP3 inflammasome activation and pathological inflammation in diabetic wound healing. *Cell Rep Med*. 2023;4(8):101129.
- Marjana TC, Jamie LB, Katelyn EO, et al. Skin microbiota and its interplay with wound healing. *Am J Clin Dermatol*. 2020;21(Suppl 1):36–43.
- Bharati KP, Kadamb HP, Ryan YH, et al. The gut-skin microbiota axis and its role in diabetic wound healing-a review based on current literature. *Int J Mol Sci*. 2022;23(4):2375.
- Seddik HA, Bendali F, Gancel F, et al. Lactobacillus plantarum and its probiotic and food potentialities. *Probiotics Antimicrob Proteins*. 2017;9(2):111–122.
- Mohtashami M, Mohamadi M, Mohsen AN, et al. Lactobacillus bulgaricus and lactobacillus plantarum improve diabetic wound healing through modulating inflammatory factors. *Biotechnol Appl Biochem*. 2021;68(6):1421–1431.
- Tsai WH, Chou CH, Huang TY, et al. Heat-killed lactobacilli preparations promote healing in the experimental cutaneous wounds. *Cells*. 2021;10(11):3264.
- Gan Y, Chen X, Ruokun Y, et al. Antioxidative and anti-inflammatory effects of lactobacillus plantarum zs62 on alcohol-induced subacute hepatic damage. *Oxid Med Cell Longev*. 2021;2021:7337988.
- Wu Y, Hu A, Xin S, et al. Lactobacillus plantarum postbiotics trigger AMPK-dependent autophagy to suppress Salmonella intracellular infection and NLRP3 inflammasome activation. *J Cell Physiol*. 2023;238(6):1336–1353.
- Yang S, Feng Y, Chen L, et al. Disulfiram accelerates diabetic foot ulcer healing by blocking NET formation via suppressing the NLRP3/Caspase-1/GSDMD pathway. *Transl Res*. 2023;254:115–127.
- Accipe L, Abadie A, Nevier R, et al. Antioxidant activities of natural compounds from Caribbean plants to enhance diabetic wound healing. *Antioxidants*. 2023;12(5):1079.
- Zhao Y, Wang Q, Yan S, et al. Bletilla striata polysaccharide promotes diabetic wound healing through inhibition of the NLRP3 inflammasome. *Front Pharmacol*. 2021;12:659215.
- Li X, Wang T, Tao Y, et al. MF-094, a potent and selective USP30 inhibitor, accelerates diabetic wound healing by inhibiting the NLRP3 inflammasome. *Exp Cell Res*. 2022;410(2):112967.
- Kaur Sandhu S, Raut J, Kumar S, et al. Nanocurcumin and viable Lactobacillus plantarum based sponge dressing for skin wound healing. *Int J Pharm*. 2023;643:123187.
- Kim JS, Kim J, Lee SM, et al. Development of guar gum-based dual-layer wound dressing containing lactobacillus plantarum: rapid recovery and mechanically flexibility. *Int J Biol Macromol*. 2022;221:1572–1579.
- Ong JS, Taylor TD, Yong CC, et al. Lactobacillus plantarum USM8613 aids in wound healing and suppresses staphylococcus aureus infection at wound sites. *Probiotics Antimicrob Proteins*. 2020;12(1):125–137.
- Chuang YC, Cheng MC, Lee CC, et al. Effect of ethanol extract from Lactobacillus plantarum TWK10-fermented soymilk on wound healing in streptozotocin-induced diabetic rat. *AMB Express*. 2019;9(1):163.

29. Panagiotou D, Filidou E, Gaitanidou M, et al. Role of lactiplantibacillus plantarum UBLP-40, Lactobacillus rhamnosus UBLR-58 and bifidobacterium longum UBBL-64 in the wound healing process of the excisional skin. *Nutrients*. 2023;15(8):1822.
30. Wang L, Zhao Z, Zhao L, et al. Lactobacillus plantarum DP189 reduces  $\alpha$ -SYN aggravation in MPTP-induced parkinson's disease mice via regulating oxidative damage, inflammation, and gut microbiota disorder. *J Agric Food Chem*. 2022;70(4):1163–1173.
31. Zhang Y, Li Y, Wang X, et al. Lactobacillus Plantarum NC8 and its metabolite acetate alleviate type 1 diabetes via inhibiting NLRP3. *Microb Pathog*. 2023;182:106237.

## Journal of Inflammation Research

Dovepress

### Publish your work in this journal

The Journal of Inflammation Research is an international, peer-reviewed open-access journal that welcomes laboratory and clinical findings on the molecular basis, cell biology and pharmacology of inflammation including original research, reviews, symposium reports, hypothesis formation and commentaries on: acute/chronic inflammation; mediators of inflammation; cellular processes; molecular mechanisms; pharmacology and novel anti-inflammatory drugs; clinical conditions involving inflammation. The manuscript management system is completely online and includes a very quick and fair peer-review system. Visit <http://www.dovepress.com/testimonials.php> to read real quotes from published authors.

Submit your manuscript here: <https://www.dovepress.com/journal-of-inflammation-research-journal>